(Online) ISSN 2712-0562
Original Research

Sustainable Engineering and Innovation
Vol. 7, No. 2, 2025, pp.449-462
https://doi.org/10.37868/sei.v7i2.id633

Comprehensive characterization of switching and conduction losses in high-ratio step-down converters for next-generation electric vehicles

Zainab Hussam Al-Araji[1*], Muhanad D. Hashim Almawlawe[2], Musa Hadi Wali[3]
[1] Physics Department, College of Science for Women, University of Baghdad, Baghdad, Iraq
[2,3] Department of Electronics & Telecom., College of Engineering, University of Al-Qadisiyah, Al-Diwaniyah, Iraq

*Corresponding author E-mail: zainab.musa@csw.uobaghdad.edu.iq

Received Mar. 22, 2025
Revised Sep. 02, 2025
Accepted Sep. 11, 2025
Online Sep. 25. 2025

Abstract

Sustainable energy has become a critical focus due to the environmental and economic limitations of traditional fossil fuels. One of the most prominent applications in this field is electric vehicles (EVs), which rely on high-voltage DC battery packs (typically 400V or 800V) as their primary energy source. These batteries supply power to AC motors via inverters that convert direct current (DC) to alternating current (AC). Additionally, EVs incorporate DC-DC converter systems to step down the high-voltage DC for auxiliary systems such as infotainment units, control modules, and lighting. The step-down DC-DC converter is composed of various components, including switches (such as MOSFETs or IGBTs) and diodes. These components are subject to different types of losses—namely switching, conduction, and thermal losses—which can significantly impact system efficiency and performance. This article investigates these losses through simulation using the PLECS software across multiple operating scenarios.

Keywords: Electric vehicles, switching losses, Conduction losses, Sw, Efficiency analysis, DC-DC converters

1. Introduction

Automobiles known as electric vehicles (EVs) feature one or more electric motors that operate from rechargeable battery energy storage systems [1]. EV's has several advantages over traditional internal combustion engine (ICE) vehicles such as: zero emissions (no tailpipe emissions, reducing air pollution), high efficiency (electric motors are more efficient than internal combustion engines), instant torque (EVs typically use a single-speed transmission because electric motors provide high torque across a wide range of speeds, eliminating the need for multi-gear systems), lower maintenance (fewer moving parts compared to traditional vehicles) [2, 3]. The block diagram of the EVs can be seen in Figure 1.

This research investigates the step-down DC-DC converter that lowers high voltage to provide power for auxiliary equipment such as lighting and infotainment units and control modules, together with electronics and climate control systems, and other equipment. The block diagram of the step-down converter is shown in Figure 2. [4], [5].

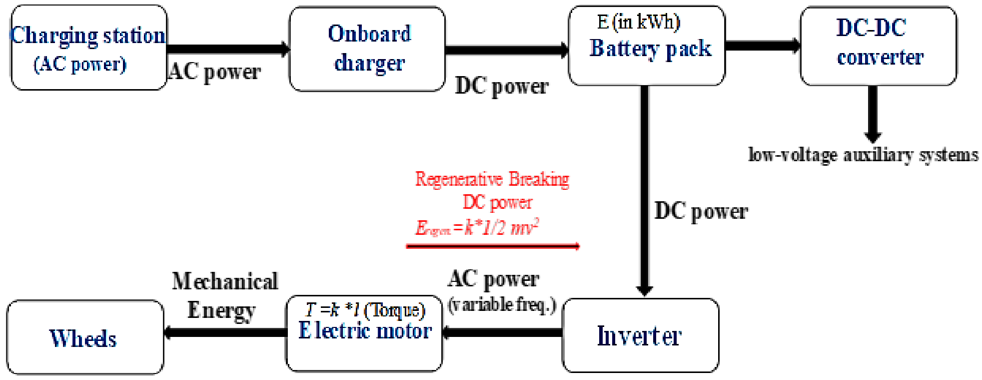

Figure 1. Block diagram of the EV

The operation of a buck converter can be divided into two states:

1. On-state (D × T_s): The high-side MOSFET is turned on, connecting the input voltage to the inductor. The inductor current increases linearly, storing energy.
2. Off-state ((1-D) × T_s): The high-side MOSFET is turned off, and the low-side MOSFET (or diode) conducts. The inductor current decreases linearly, transferring.

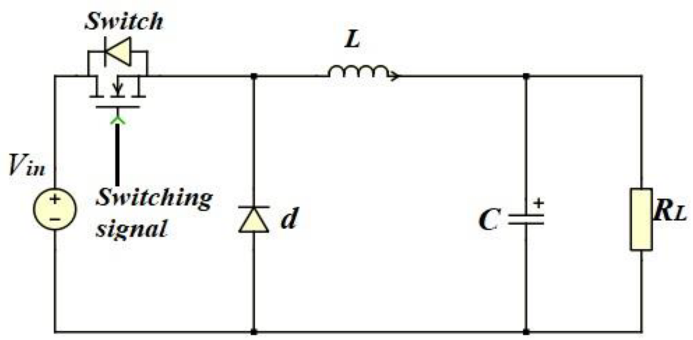

Figure 2. Step-down DC-DC converter

The efficiency of a step-down converter is influenced by various types of energy losses that occur during the conversion process, which can be categorized into conduction losses, switching losses, and core losses. Conduction losses arise from the resistive elements in the circuit, such as the equivalent series resistance (ESR) of the inductor and capacitor, and the on-resistance (RDS (on)) of the switching transistor (typically a MOSFET or IGBT). These losses are proportional to the square of the current (I^2*R) and dominate at higher load conditions. Switching losses, on the other hand, occur during the transition phases when the switch toggles between the on and off states. These losses are associated with the overlap of voltage and current during switching transitions, leading to power dissipation in the form of heat. The switching frequency is also a critical factor; the bigger the passive components are, the more the switching losses are; the switching frequency is higher, and the losses occur more often.

The core of an inductor is subject to two primary types of losses: hysteresis losses and eddy current losses, which behave differently in response to changing operating conditions. These losses become particularly significant at high operating frequencies, where efficiency is affected by both magnetic and switching losses [6]. Hysteresis losses depend on the magnetic properties of the core material and increase with frequency, while eddy current losses are caused by circulating currents induced within the core material, which also scale with frequency and material conductivity [7], [8].

To mitigate these losses, modern inductors often use advanced ferrite materials with low core loss characteristics. Additionally, wide-bandgap semiconductors such as silicon carbide (SiC) and gallium nitride (GaN) are increasingly used in power switches due to their lower switching losses and superior thermal conductivity [9], [10]. These material and component improvements play a critical role in enhancing the overall efficiency of step-down (buck) converters, which typically achieve efficiencies in the range of 90–98% in modern designs.

2. Literature review

A prototype step-down converter 200 V input and, 24V 10A output was built in [6] to check the theory examination findings. The report gives information regarding operational functions and practical evidence. The converter proposed has lower operational voltages compared to other IBCs, as well as high step-down capabilities. The converter has a good performance in high power applications due to the fact that it provides. A non-isolated step-down operating parameter, along with low output current ripple and constant input current behavior. The study compares the algorithm checking and performance of the converter with the aid of theory and experimental evidence. The building of a balanced assessment consists of the examination of constraints along with implementation issues and alternative solutions in which the proposed converter is performing inadequately. This aspect will be lacking, and the results will remain biased in the evaluation.

In [7], conventional boost converters (CBCs) are compared to flying capacitor boost and discuss converters (FCBCs) and multilevel boost converters with an emphasis on their advantages and disadvantages. An FCBC delivers significantly greater ratios of voltage conversion compared to its counterpart CBC with the same duty cycle. The increased voltage output limits with FCBCs are due to reduced duty cycle limits, which could retard system behavior and reduce power switching loss. The diminished physical dimensions of FCBC. Inductors versus CBC inductors will result in a smaller weight and size, and lower cost, along with reduced weight of inductors, copper losses. The lifecycle of the output signals is passed through various stages in FCBC, which leads to reduced EMI. Complex design, along with control of FCBCs, increases production costs because their multiple components and intricate synchronization system demand additional complexity. Multiple switching stages decrease the overall efficiency levels of FCBCs. Multiple components in such systems typically generate more parasitic losses, which reduces total system efficiency. In summary, FCBCs offer enhanced voltage conversion and reduced inductor size but at the cost of increased complexity, cost, and potentially lower efficiency compared to CBCs.

Study in [8] allows designers to calculate the total dynamic power loss in a buck converter using static characteristics and device parameters from datasheets. This enables optimization of device operation within the circuit. It investigates the dynamic power loss in a buck converter and offers several benefits, such as the key advantage of proposing a transient analytic model for calculating transient loss, incorporating significant parasitic parameters often overlooked in the past. However, a potential drawback is the document's specific focus on buck converters, which may limit its applicability to other types of converters. Additionally, relying on datasheet parameters may introduce inaccuracies if the datasheet information is incomplete or not representative of real-world conditions. The complexity of the proposed model could also be a barrier for designers unfamiliar with advanced power electronics analysis techniques.

Study in [9] aims to provide an overview of thermal transport mechanisms at high temperatures, identify challenges, and explore material research opportunities for high-temperature thermal materials. Many drawbacks may be of interest in this document, like challenges in obtaining empirical data for high-temperature thermal properties, which could limit the robustness of conclusions drawn in the paper. Integrating insights from related fields (like low-temperature phenomena), it may lack a holistic view of thermal transport science.

Study in [12] identifies where the greatest power losses occur in electric vehicles, allowing for targeted improvements in energy efficiency. It presents methodologies to optimize the operating points of key components such as the electric motor, inverter, and mechanical transmission, enhancing overall vehicle performance. Also, the document offers efficiency curves that can serve as a reference for manufacturers and engineers to improve design and functionality in future electric vehicle models. The main drawbacks of this paper may include: limited scope of analysis, specific test environment, lack of economic analysis, and focus on efficiency without consideration of other factors. Moreover, research by [14] evaluates the performance characteristics of a 1 kW Asynchronous Buck Converter (ASBC) and a Synchronous Buck Converter (SBC) as electric vehicle battery chargers. The article provides a comprehensive analysis of the computation of the IGBT power loss in the electric vehicle charging applications and thermal stability study. Figure 3 indicates that a 5A load current value will eventually stabilize the thermal distribution in the designed heatsink (IGBT) to 36.20 and 42.50 with ASBC and SBC counterparts operating, respectively.

The study in [15] was conducted by a team of researchers who made an effort to design thermal control methods that ensure the reliability of power electronic converters and extended lifetime operation. The heat dissipating control system is controlled actively by cooling, employing direct or indirect methods to control electrical quantities and resist temperature. A few of the cooling processes mentioned in this study are channel cooling and phase change material-based cooling and immersion cooling, and jet cooling. They were practically applied and were successful in the impregnation and spray cooling.

3. Theoretical analysis

3.1. Step-down DC/DC converter

Step-down DC-DC converter mathematical calculations determine the link between all input and output values and other crucial parameters. The conversion process depends on essential mathematical evaluations, which enable necessary design steps and performance optimization of the converter for electric vehicle applications. The following section contains a complete mathematical breakdown of buck converter operations [16, 17]:

$$
\begin{aligned}
D &= \frac{V_{out}}{V_{in}} \\
\eta &= \frac{P_{out}}{P_{in}} \\
L &= \frac{V_{out}\left(V_{in}-V_{out}\right)}{V_{in} * f_s * \Delta I_L} \\
C &= \frac{\Delta I_L}{8 * f_s * \Delta V_{out}}
\end{aligned}
\tag{1}
$$

Where:

D - Duty cycle, L - inductor value, V_{in} - Input voltage, V_{out} - Output voltage, fs - Switching frequency, ΔI_L - Current ripple, C - capacitor value, ΔV_{out} - Voltage ripple, η - efficiency.

3.2. Losses mechanism analysis

Understanding loss mechanisms in step-down DC-DC converters used in electric vehicles is essential for improving system efficiency and increasing vehicle range. The main challenge in 400V to 12V applications is the high conversion ratio that leads to a low duty cycle and significant switching losses. Efficiency can be improved through appropriate device selection, application of advanced switching techniques, and consideration of alternative designs such as multi-phase or cascaded converters. These losses can be categorized into several key components, including conduction losses, switching losses, and parasitic losses.

Conduction losses primarily originate from the resistance of the inductor and the on-state resistance of the activated MOSFET. These losses, along with the forward-voltage drop across the diode, collectively contribute to the total conduction losses. Since these losses are proportional to the square of the current, they become particularly significant under high load conditions.

Switching losses occur during the transition states of the transistors—when the MOSFET and the diode shift between on and off states. These losses are influenced by switching frequency and gate drive characteristics and become more pronounced at higher frequencies. Parasitic losses, such as those caused by the equivalent series resistance (ESR) of output capacitors, also contribute to overall inefficiency [11], [12]. Additional losses include the diode's reverse recovery charge and other circuit parasitics.

The total power loss in a step-down converter reflects the combined effects of these various sources, establishing a quantitative relationship among them [13], [14]. Therefore, optimizing the design parameters—such as selecting appropriate semiconductor devices, defining suitable inductor specifications, and determining optimal switching frequencies—is essential to minimize individual loss components [15], [16].

Effective design optimization of semiconductors, inductors, and switching behavior directly leads to reduced power losses and improved converter efficiency. This optimization is crucial for extending the driving range of electric vehicles (EVs), which increasingly demand enhancements in power handling and energy utilization. As a result, this area remains a major focus of current research and development in sustainable transportation technologies [17]–[19].

Conduction losses

$$P_{swit.cond} = I_{out}^2 * R_{DS(on)}; \tag{2}$$

Where: I_{out} – Output current, $R_{DS(on)}$ - the on-resistance of the MOSFET or IGBT.

Inductor conduction loss

$$P_{ind.cond} = I_{out}^2 * R_L; \tag{3}$$

Switching losses

$$P_{switch} = \frac{1}{2} * V_{in} * I_{on} * f_s * t_r; \tag{4}$$

Where: tr - the rise time of the switch.

Core losses

$$P_{core} = k_h * f_s^n + *k_e * f_s^2; \tag{5}$$

Where: kh and ke are material-dependent constants, and n depends on the magnetic material. These various losses are represented in Figure 3, where the vertical axis represents the power loss in watts (W), while the horizontal axis represents the different loss components. In Figure 4, thermal losses for various components used in the step-down converter are represented.

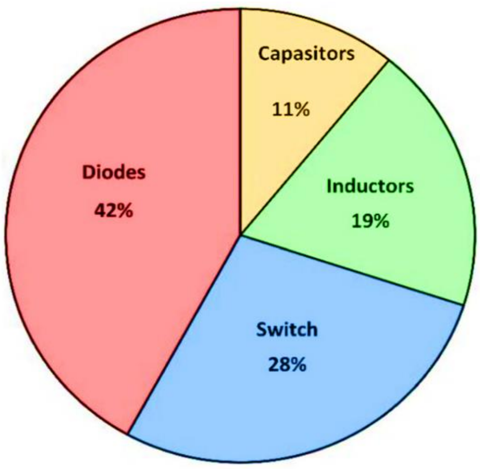

Figure 3. Various losses of the step-down converter

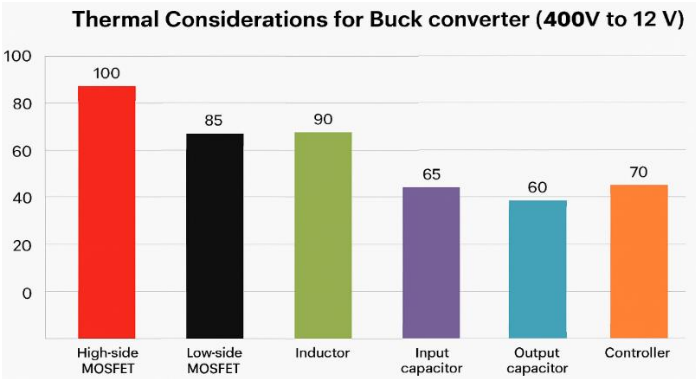

Figure 4. Thermal losses of different components of the step-down converter

4. Results and discussion

This section is particularly important, as it demonstrates how the converter meets the stringent reliability, safety, and compatibility requirements of the automotive industry. The calculation values adopted in previous section is considered in this section which involves the inductor value, capacitor value, semiconductor selection (high-side IGBT: with 650V rating, low RDS(on) (≈100mΩ), and optimized gate charge characteristics like IKWH70N65WR6-IGBT, low-side IGBT: low-voltage (80-100V) with ultra-low RDS(on) (≈3-5mΩ) to minimize conduction losses during the long off-time of the high-side switch). The main components of the buck converter are given in Table 1. In Figure 5, the simulation model of the buck converter using PLECS software is considered.

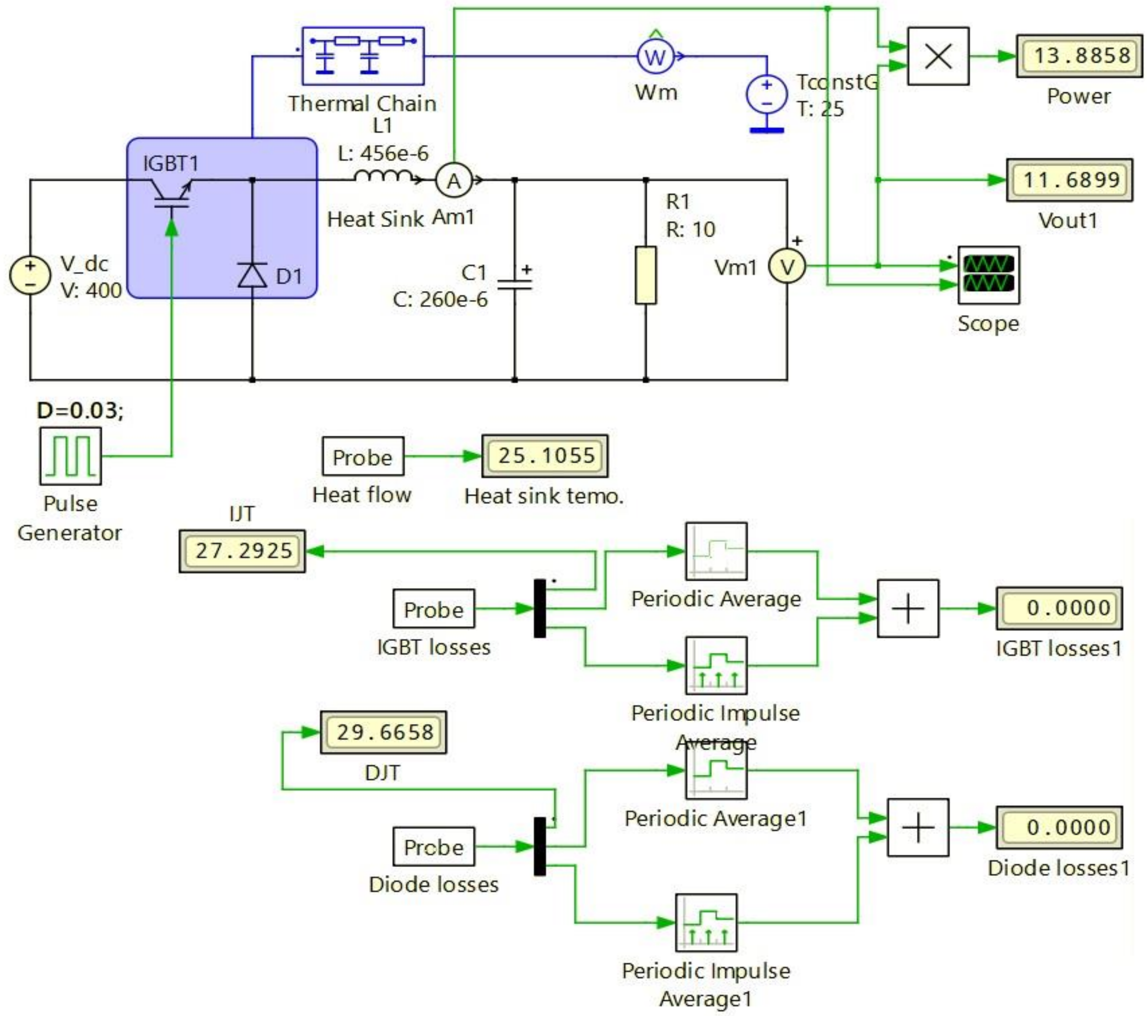

Figure 5. Schematic diagram of a step-down converter with the losses instrumentation

Table 1. Main components of the buck converter

Component	Symbol	Value
Input voltage	V_dc	400V
Output voltage	Vout	12V
Inductor	L1	100mH
Capacitor	C1	260µF
Output resistor	R1	10Ω
Switching freq.	fsw	5-100 kHz

Figure 6 illustrates the output voltage and inductor current of the step-down converter with different switching frequencies (5, 10, 50, 100) kHz. The provided waveforms offer valuable insights into the performance of the step-down DC-DC converter in electric vehicle applications when converting 400V to 12V. The waveforms show that increasing the operating frequency improves dynamic performance and reduces output ripple, with challenges in transient response and high conversion ratio. The converter's performance can be improved through advanced control techniques and by selecting the optimal frequency that balances performance and efficiency. The switching and conduction losses can be calculated using Equations 2 and 4. Table 2 summarizes these losses in the step-down converter considered in this article with respect to different frequencies.

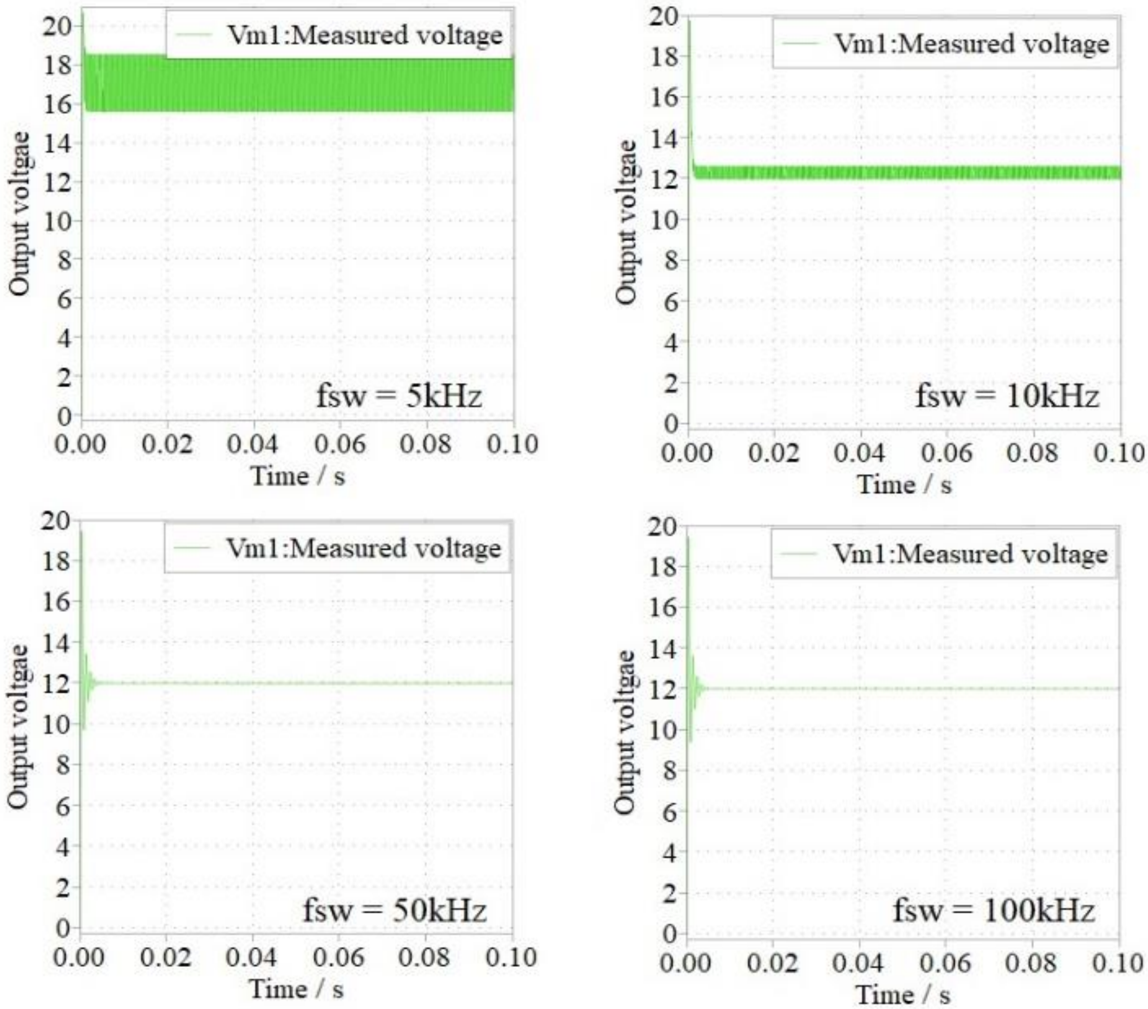

Figure 6. Simulation process of the step-down converter under different switching frequencies

Table 2. Summarized values due to calculations

Switching losses(W)	Conduction losses(W)	Efficiency (%)	Voltage ripple (V)	Switching Freq.
0.03	3.4	94.6	0.12	10000
0.06	3.4	94.55	0.12	20000
0.1	3.4	94.5	0.12	30000
0.13	3.4	94.45	0.12	40000
0.16	3.4	94.4	0.12	50000
0.19	3.4	94.35	0.12	60000
0.23	3.4	94.31	0.12	70000
0.26	3.4	94.26	0.12	80000
0.29	3.4	94.21	0.12	90000
0.32	3.4	94.16	0.12	100000

Using Table 2, the switching and conduction losses calculated for the step-down DC-DC converter can be mapped in Figure 7.

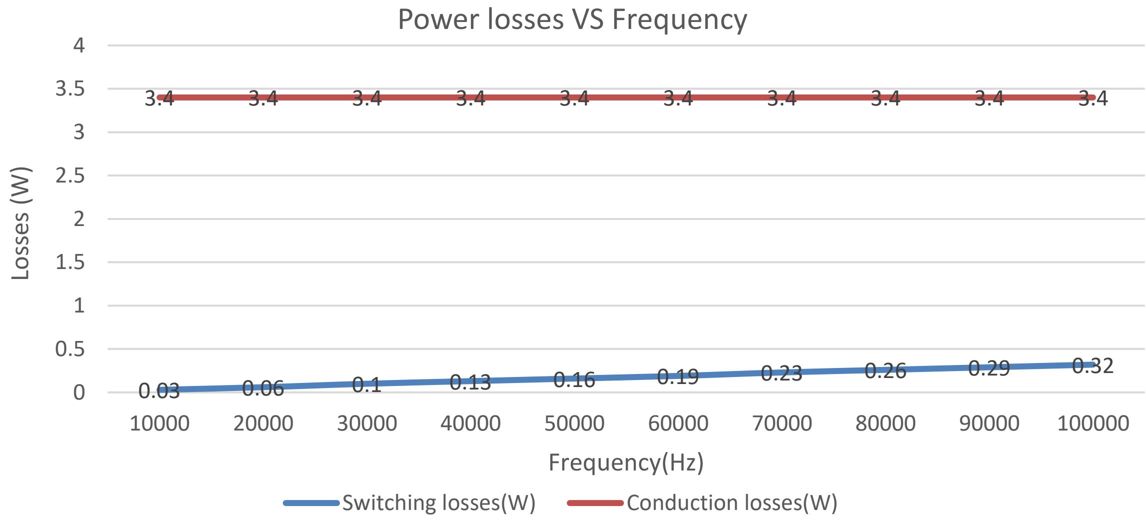

Figure 7. Switching and conduction losses VS switching frequency

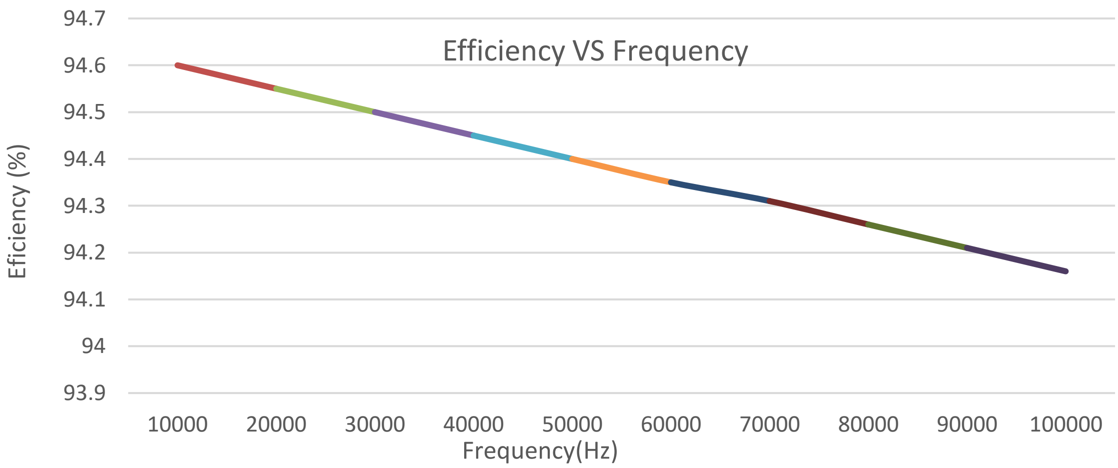

Figure 8. Efficiency VS switching frequency in a step-down converter

The efficiency can be illustrated from another view, or the efficiency against load current, as it is shown in Figure 9.

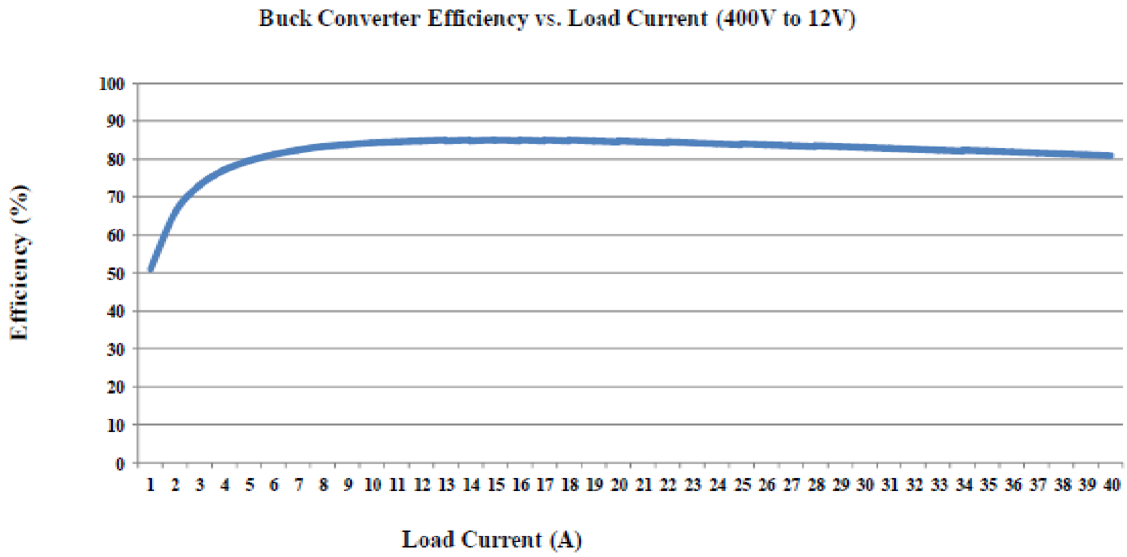

Figure 9. Step-down converter efficiency analysis alongside its relation to load current

Another simulation attempt is considered in Figure 10, which describes the relationship between efficiency and input.

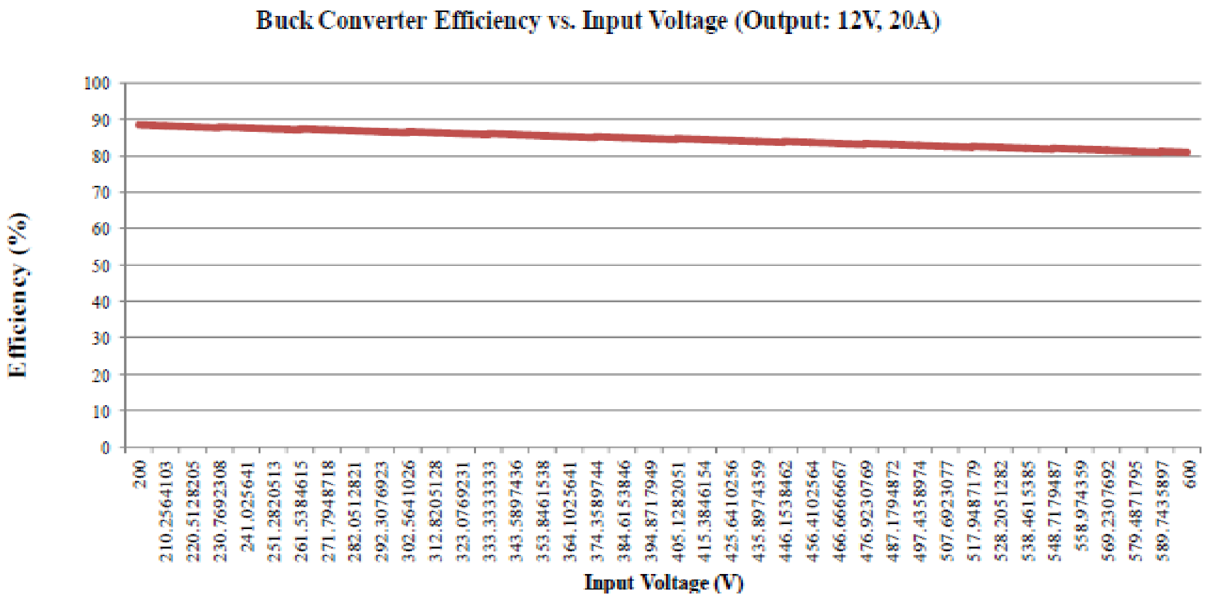

Figure 10. Efficiency VS input voltage in a step-down converter

The simulation results of the step-down DC-DC converter demonstrate several key performance characteristics across different operating conditions. Figure 7 illustrates the output voltage waveforms at various switching frequencies (10, 50, 75, and 100 kHz). As the switching frequency increases, there is a notable improvement in the dynamic performance of the converter, characterized by reduced output voltage ripple. This improvement is significant for automotive applications where a stable voltage supply to auxiliary systems is critical for reliable operation. The analysis of loss mechanisms reveals the distribution of power losses across different components of the converter. As shown in Figure 3, the total power loss is comprised of several components, with conduction and switching losses being the most significant contributors. The analysis of the thermal data in Figure 4 further illustrates how these losses are converted into thermal gains in various parts, which is crucial for thermal management and reliability concerns in automotive systems.

Table 2 shows the switching and conduction losses at various operating frequencies computed. The following calculations were done based on the mathematical models provided in the section on methodology: Conduction losses:

$$\begin{aligned} &Conduction\ losses = I_{out}^2 * R_{DS(on)} * D; \\ &Switching\ losses = 0.5 * V_{in} * I_{out} * t_r * f_s. \end{aligned} \quad (6)$$

These losses, along with the switching frequency, are graphically illustrated in Figure 7. The results indicate that switching losses increase proportionally with frequency, while conduction losses remain relatively constant across the frequency range. This linear relationship between switching frequency and switching losses aligns with theoretical expectations, as higher frequencies lead to more frequent transitions in the semiconductor devices, thereby increasing energy loss. In contrast, conduction losses are primarily influenced by the on-state resistance of the semiconductor devices and the magnitude of the current, making them largely independent of switching frequency.

The step-down converter was tested in varying operating conditions to offer efficiency and in-depth knowledge of its performance behavior. Figure 8 shows the correlation between switching frequency and efficiency. The findings indicate that efficiency is reduced with an increase in the switch frequency, which can be explained by higher switching losses at higher frequencies. This trade-off between switching frequency and efficiency is a critical consideration in the design of DC-DC converters for electric vehicles, where both high efficiency and compact size (enabled by higher switching frequencies) are desirable. The efficiency versus load current relationship, presented in Figure 9, demonstrates that the converter achieves its peak efficiency at moderate load currents. At light loads, the fixed losses (such as gate drive losses and core losses) become proportionally significant, reducing overall efficiency. At heavy loads, the I^2R losses in the semiconductor devices and passive components increase quadratically with current, also reducing efficiency. Figure 10 shows the efficiency as a function of input voltage. The results indicate that the converter maintains relatively stable efficiency across the input voltage range, which is important for electric vehicle applications where the battery voltage can vary significantly depending on the state of charge.

Under simulated operating conditions, the selected components IKWH70N65WR6 for high-side IGBT and low-side IGBT showed suitable temperatures as per thermal analysis. The ability to maintain stable temperatures in high-temperature environments serves as an essential attribute for automotive converter reliability, as automotive environments pose harsh conditions that can lead to severe component failure effects.

The simulation results demonstrate a balanced trade-off between switching frequency and key performance metrics in a 400V to 12V step-down DC-DC converter. As the switching frequency increases—particularly within the 10 kHz to 100 kHz range—both output voltage ripple and dynamic response show significant improvements. This enhanced dynamic behavior supports stable voltage delivery to auxiliary systems in electric vehicles.

However, these performance gains come at the cost of increased switching losses, which negatively affect overall converter efficiency. This presents a fundamental design challenge in power electronics for EVs: the trade-off between high-frequency performance benefits and energy efficiency.

Higher switching frequencies enable the use of smaller passive components, such as inductors and capacitors, thereby reducing the size, weight, and cost of power converters—an important advantage in space-constrained and weight-sensitive automotive applications, especially for autonomous and compact EV designs. In such cases, minimizing component size contributes directly to extended driving range and improved vehicle performance. Lower efficiency at higher switching frequencies can offset these benefits by requiring more robust thermal management systems and potentially larger components to handle the resulting heat, which may in turn reduce overall vehicle range.

Therefore, selecting the optimal switching frequency must account for the specific requirements and constraints of the EV design. In applications where energy efficiency and battery conservation are critical, lower switching frequencies are preferable. In contrast, applications prioritizing size and weight optimization may benefit from higher switching frequencies, provided the efficiency trade-offs are acceptable. Ultimately, the ideal switching frequency is context-dependent, based on a careful evaluation of performance priorities and system limitations.

The simulation process demonstrates that conduction losses maintain similar levels throughout the testing period. The frequency range produces a steady conduction loss rate, but switching losses rise in direct proportion to frequency. The characteristics of efficiency for different operating conditions enable the researchers to make valuable conclusions related to practical applications. This reduction in efficiency with the number of switching times requires proper selection of the operating frequency, which is equally essential since it affects the devices' performance. The load current vs efficiency relationship deduces that the power converter values off to its peak operating value where the converter operates in medium levels of power; therefore, the auxiliary load in electric vehicles adopts varying values during operation.

Considering the efficiency curve, which can provide more precise predictions of the converter operation in real-world considerations. There is not much difference in the converter's efficiency when it is run over the given range of the input voltage. Experiments on the device in actual operating conditions can determine methods for regulating loads that would be most efficient for the system. In electric vehicles, the converter performs well since the voltage in batteries varies in extreme values. The level of charge determines the level of fluctuation of the voltage of the battery, and this is 20% or more, depending on the state selected. The converter is stable, as also verified by the efficiency measurement. The 400 V to 12 V converter in question compares favorably in terms of performance with the traditional step-down converters, defined in the article, both in power density and power efficiency. Even though it was of a high conversion ratio (33.3:1), the design possesses unique issues that cannot be addressed by single-stage buck converters along with this design. A number of steps in a cascaded or series type shall provide better output efficiency in converting 400 V to 12 V because the process of conversion is divided into various steps, which operate with maximum duty cycles. The parameters of the present study can be enhanced with the help of microstrip filters [21, 22], antennas [20, 24], AI methods [25, 26], and wireless networks [27, 28].

5. Conclusion

This article analyzes in detail a 400V to 12V step-down DC-DC converter for electric vehicle auxiliary systems. Electric vehicle auxiliary systems, with particular focus on loss mechanisms and performance optimization across various operating conditions. Through systematic PLECS simulations with switching frequency range from 10 kHz to 100 kHz, an important relationship is found between operating parameters and converter efficiency that defines the converter performance. The efficiency of EV power systems depends heavily on operating parameter relationships, which require analysis for design purposes. The analysis demonstrates that converters have to balance between different switching frequency settings. The dynamic response and output voltage performance of the system are optimized through high-frequency operation between 75-100 kHz. The improved power quality perception provides essential benefits to sensitive automotive electronics. However, this improvement decreases efficiency when switching losses elevate during operation. In contrast, lower frequencies (10-30 kHz) increase the efficiency range of these converters but imply large passive components, which result in weight and space requirements based on converter size and weight.

6. Future works

Future research in high-step-down DC-DC converters should focus on analyzing alternative topologies capable of achieving large voltage conversion ratios. Notable examples include tapped-inductor buck converters and hybrid switched capacitor/inductor-based converters. These topologies offer potential performance improvements; however, realizing their full benefits, especially at high switching frequencies, remains a challenge, even with advanced wide-bandgap devices such as SiC and GaN. Nonetheless, these technologies represent a promising direction for future development. Adaptive control strategies also show strong potential for optimizing converter performance by dynamically adjusting operating parameters based on real-time load conditions and temperature measurements. Such control approaches could significantly enhance efficiency and responsiveness.

To ensure long-term reliability in automotive environments, rigorous testing and reliability assessments must be conducted. Components must withstand harsh conditions, including repeated thermal cycling and other environmental stresses typical of vehicular applications. The proposed research directions aim to improve the performance, power density, and reliability of step-down converters in electric vehicles. These advancements are critical for the continued evolution of EV technology, supporting greater energy efficiency, compact design, and extended vehicle range.

Declaration of competing interest

The authors declare that they have no known financial or non-financial competing interests in any material discussed in this paper.

Funding information

The author declares that they have received no funding from any financial organization to conduct this research.

Author contribution

Zainab Hussam Al-Araji: Conceptualization of the study, design, and writing of the original draft.

Muhanad D. Hashim Almawlawe: Conducted simulations and analysis of the filter performance, contributed to the methodology, and assisted in manuscript preparation.

Musa Hadi Wali: Provided insights into the design process, performed experimental validation, and contributed to the discussion of results.

References

[1] C. Zimm, "Improving the understanding of electric vehicle technology and policy diffusion across countries," *Transp. Policy*, vol. 105, pp. 54–66, 2021. https://doi.org/10.1016/j.tranpol.2020.12.012

[2] N. Kittner, et al., "Electric vehicles," in *Technological Learning in the Transition to a Low-Carbon Energy System*, Academic Press, 2020, pp. 145–163. https://doi.org/10.1016/B978-0-12-818762-3.00009-1

[3] D. S. Rapson and E. Muehlegger, "The economics of electric vehicles," *Rev. Environ. Econ. Policy*, vol. 17, no. 2, pp. 274–294, 2023. https://doi.org/10.1086/725484

[4] H.-H. Chou and H.-L. Chen, "A novel buck converter with constant frequency controlled technique," *Energies*, vol. 14, no. 18, p. 5911, 2021. https://doi.org/10.3390/en14185911

[5] D. Mitić, et al., "Input-output based quasi-sliding mode control of DC-DC converter," *Facta Univ. Ser. Electron. Energ.*, vol. 25, no. 1, pp. 69–80, 2012. https://doi.org/10.2298/FUEE1201069M

[6] M. Esteki, et al., "Interleaved buck converter with continuous input current, extremely low output current ripple, low switching losses, and improved step-down conversion ratio," *IEEE Trans. Ind. Electron.*, vol. 62, no. 8, pp. 4769–4776, 2015. https://doi.org/10.1109/TIE.2015.2397881

[7] M. D. H. Almawlawe, H. H. Naji, I. H. A. Al_Umari, and M. H. Wali, "Enhanced voltage conversion and reduced inductor size in a flying capacitor boost converter compared to a conventional boost converter for photovoltaic systems," *Al-Qadisiyah J. Eng. Sci.*, vol. 17, pp. 322–330, 2024.

[8] W. Zhang, et al., "The dynamic power loss analysis in buck converter," in *Proc. IEEE 6th Int. Power Electron. Motion Control Conf.*, 2009, pp. 362–367. https://doi.org/10.1109/IPEMC.2009.5157413

[9] S. Shin, et al., "Advanced materials for high-temperature thermal transport," *Adv. Funct. Mater.*, vol. 30, no. 8, p. 1904815, 2020. https://doi.org/10.1002/adfm.201904815

[10] C. B. O'Neal, et al., "Advanced materials for high temperature, high performance, wide bandgap power modules," *J. Electron. Mater.*, vol. 45, no. 1, pp. 245–254, 2016. https://doi.org/10.1007/s11664-015-4187-5

[11] S. M. Abd El-Azeem and S. M. El-Ghanam, "Comparative study of gallium nitride and silicon carbide MOSFETs as power switching applications under cryogenic conditions," *Cryogenics*, vol. 107, p. 103071, 2020. https://doi.org/10.1016/j.cryogenics.2020.103071

[12] J. D. Valladolid, et al., "Experimental performance evaluation of electric vehicles (EV) based on analysis of power and torque losses," in *Proc. IEEE Int. Conf. Ind. Technol. (ICIT)*, 2020, pp. 933–938. https://doi.org/10.1109/ICIT45562.2020.9067241

[13] A. Garg and M. Das, "High efficiency three-phase interleaved buck converter for fast charging of EV," in *Proc. IEEE Int. Conf. Power Electron. Energy (ICPEE)*, 2021, pp. 1–5. https://doi.org/10.1109/ICPEE50452.2021.9358486

[14] M. R. Haque, et al., "Analysis of loss profile and thermal distribution of heat sink of IGBT-based asynchronous and synchronous buck converters for EV charging system," in *Proc. IEEE Int. Conf. Electron. Mater. Eng. Nano-Technol. (IEMENTech)*, 2021, pp. 1–6. https://doi.org/10.1109/IEMENTech53263.2021.9614827

[15] S. M. I. Rahman, et al., "Emerging trends and challenges in thermal management of power electronic converters: A state of the art review," *IEEE Access*, vol. 12, pp. 50633–50672, 2024. https://doi.org/10.1109/ACCESS.2024.3385429

[16] R. Kaur and S. Kumar, "Stability and dynamic characteristics analysis of DC-DC buck converter via mathematical modelling," in *Proc. IEEE Int. Conf. Recent Dev. Control Autom. Power Eng. (RDCAPE)*, 2015, pp. 253–258. https://doi.org/10.1109/RDCAPE.2015.7281405

[17] J. Lee, "Basic calculation of a buck converter's power stage," *Appl. Note AN041*, Richtek Technology Corp., pp. 1–8, 2015.

[18] A. W. Cristri and R. F. Iskandar, "Analysis and design of dynamic buck converter with change in value of load impedance," *Procedia Eng.*, vol. 170, pp. 398–403, 2017. https://doi.org/10.1016/j.proeng.2017.03.064

[19] U. Gupta and A. Vass-Varnai, "Design of buck converter with control system for electric vehicle using SiC device with thermal loss model," in *Proc. Int. Electron. Packag. Tech. Conf. Exhib.*, ASME, 2022, p. V001T09A007.

[20] D. Nayanasiri and Y. Li, "Step-down DC–DC converters: An overview and outlook," *Electronics*, vol. 11, no. 11, p. 1693, 2022. https://doi.org/10.3390/electronics11111693

[21] Y. S. Mezaal, H. T. Eyyuboglu, and J. K. Ali, "New dual band dual-mode microstrip patch bandpass filter designs based on Sierpinski fractal geometry," in Proc. 2013 3rd Int. Conf. Adv. Comput. Commun. Technol. (ACCT), Rohtak, India, pp. 348–352, 2013.

[22] K. Al-Majdi and Y. S. Mezaal, "New miniature narrow band microstrip diplexer for recent wireless communications," Electronics, vol. 12, no. 3, p. 716, 2023. https://doi.org/10.3390/electronics12030716

[23] A. H. Sallomi, and H. F. Khazaal, "Reconfigurable intelligent surfaces with smart antenna opportunities and challenges," in AIP Conference Proceedings, 2025, vol. 3255, no. 1: AIP Publishing LLC, p. 040009.

[24] N. Ali, A. Mohammed, A. Aliwy, and H. Khazaal, "Development and implementation of a microstrip antenna for autonomous vehicles and IoT in 5G communication systems," Journal of applied research and technology, vol. 22, no. 6, pp. 816-822, 2024.

[25] A. Aljazaery, S. A. Fattah, I. S. Nasir, and A. H. M. Alaidi, "Developing an Advanced Framework to Recognize Suspicious Vehicles Based on the Internet of Things Applications Using LOGO Net Environment."

[26] R. J. Kadhim, F. S. Al-Juboori, and H. J. N. Alsaedi, “Driven gamification by AI in a time series healthcare case study: Statistical intervention analysis,” Sustainable Engineering and Innovation, vol. 7, no. 2, pp. 345–354, 2025. https://doi.org/10.37868/sei.v7i2.id560

[27] J. A. Aldhaibani , M. Q. Mohammed , A. A. Mahmood and M. Sellab Hamza, “Development of wearable textile patch antenna 2.43 GHz for biomedical applications,” Int. J. Adv. Technol. Eng. Explor., vol. 11, no. 111, pp. 2394–7454, 2024. https://doi.org/10.19101/IJATEE.2023.10102312

[28] J. A. Aldhaibaini, A. Yahya, R. B. Ahmad, A. S. Md Zain, and M. K. Salman, “Performance analysis of two-way multi-user with balance transmitted power of relay in LTE-A cellular networks,” J. Theor. Appl. Inf. Technol., vol. 51, no. 2, pp. 182–190, May 2013.